# Proteomic Study and Marker Protein Identification of *Caenorhabditis elegans* Lipid Droplets*[S]

**Peng Zhang‡§‡‡, Huimin Na‡§‡‡, Zhenglong Liu¶, Shuyan Zhang‡, Peng Xue‡, Yong Chen‡, Jing Pu‡§, Gong Peng‡§, Xun Huang¶, Fuquan Yang‡, Zhensheng Xie‡, Tao Xu‡, Pingyong Xu‡, Guangshuo Ou‡, Shaobing O. Zhang‖**, and Pingsheng Liu‡****

**Lipid droplets (LDs) are a neutral lipid storage organelle that is conserved across almost all species. Many metabolic syndromes are directly linked to the over-storage of neutral lipids in LDs. The study of LDs in *Caenorhabditis elegans* (*C. elegans*) has been difficult because of the lack of specific LD marker proteins. Here we report the purification and proteomic analysis of *C. elegans* lipid droplets for the first time. We identified 306 proteins, 63% of these proteins were previously known to be LD-proteins, suggesting a similarity between mammalian and *C. elegans* LDs. Using morphological and biochemical analyses, we show that short-chain dehydrogenase, DHS-3 is almost exclusively localized on *C. elegans* LDs, indicating that it can be used as a LD marker protein in *C. elegans*. These results will facilitate further mechanistic studies of LDs in this powerful genetic system, *C. elegans*. *Molecular & Cellular Proteomics 11: 10.1074/mcp.M111.016345, 317–328, 2012.***

Cells store neutral lipids in lipid droplets (LDs)[1]. Recent studies demonstrate that LDs are heterogeneous and dynamic in size and metabolic state (1–5). Moreover, studies, especially proteomic studies, have uncovered a large set of proteins that bind to the surface of LDs. Functional studies have yielded insights into, or implied how some of these proteins regulate the dynamic metabolic state of LDs (6–8).

Early studies on mammalian cells identified the PAT family proteins, now renamed as PLIN 1–5 (9), as the major LD-proteins. With PLINs as marker proteins, advances in the purification of LDs and proteomics have made possible the identification of most if not all LD-associated proteins. Such study was conducted in the budding yeast *Saccharomyces cerevisiae* and identified many lipid metabolism enzymes (10). A similar study was conducted using mammary gland cells and the protein profile of LDs was almost identical to that of the milk fat globule membrane (11). As a result of a better purification method, later studies of LDs in Chinese hamster ovary (CHO) cells discovered many functional proteins that are involved in lipid synthesis, membrane trafficking, signal transduction, and protein degradation (12). Similar findings were soon reported using HuH7 cells, 3T3-L1 adipocytes, and A-431 cells (13–15). The first comprehensive LD proteomic study of CHO cells identified 125 proteins, seven phosphorylated proteins, and several dynamic proteins such as Arf1 and its coatomers (16). In addition, a detailed lipidomic study was carried out using purified LDs (17). In genetically altered *Drosophila* strains with distinct fat metabolic activities, and in different *Drosophila* cell types, LD-protein compositions are different (18, 19). These works suggest that LDs are not simply fat storage inclusions, but rather that they are active cellular organelles (20).

The genetic model organism *C. elegans* is an attractive system for studying LDs and fat metabolism because of its advantages such as its mutations that are used as genetic tools, it is a simple system with about 1000 cells, it is easily to grown and examined, and there is accumulated data from previous studies. Through combined genetic, biochemical, and imaging approaches, *Caenorhabditis elegans* has recently been shown to utilize LDs rather than lysosome-related organelles (LROs) to store fat (21, 22). This work clarified the question of the organelle nature of *C. elegans* fat-storage structures and provided conceptual support for the notion that post-fix Nile Red/Oil Red O staining serves as a more accurate proxy for fat levels in *C. elegans* than vital Nile Red/BODIPY staining (23–25).

The structural LD-proteins, the PLINs, are expressed in eukaryotes from humans through to *Drosophila*. However, there are no genes for apparent PLIN homologs in the *C. elegans* genome, raising the question whether *C. elegans* LDs and higher eukaryotic LDs share conserved proteins and

From the ‡Institute of Biophysics, Chinese Academy of Sciences, Beijing, 100101, China; §Graduate University of Chinese Academy of Sciences, Beijing, 100049, China; ¶Institute of Genetics and Developmental Biology, Chinese Academy of Sciences, Beijing, 100101, China; ‖College of Life Sciences, Capital Normal University, Beijing, 100048, China

Received December 5, 2011, and in revised form, March 29, 2012
Published, MCP Papers in Press, April 9, 2012, DOI 10.1074/mcp.M111.016345

[1] The abbreviations used are: LD, lipid droplet; CHO, Chinese hamster ovary; PNS, postnuclear supernatant; TAG, triacylglycerol; TLC, thin layer chromatography.

mechanisms of regulation. Identifying *C. elegans* LD-proteins by biochemical purification and proteomic studies is necessary to address this question. *C. elegans* LDs, which are free of LRO contamination, have previously been isolated using a density centrifugation approach (22), however, the quantity and purity of the isolated LDs were not tested for further proteomic studies. Therefore, it is critical for lipid metabolic study using *C. elegans* to purify high quality and quantity LDs, analyze their proteome, and identify their marker proteins.

In order to identify *C. elegans* LD-proteins, especially some specific marker proteins, we developed a purification method based on our previous work (12, 17, 22) to purify LDs from this organism. Proteomic analysis identified 306 proteins, including 193 proteins that were previously found to be present in the LD proteomes of other organisms. Through both *in vivo* imaging and *in vitro* biochemical approaches, we found that DHS-3 is localized and highly enriched on the surface of LDs, indicating that it can be used as a specific marker protein for LDs in *C. elegans*.

## EXPERIMENTAL PROCEDURES

*Materials*—A Colloidal Blue stain kit was purchased from Invitrogen (Carlsbad, CA). PDH-E1$\alpha$ monoclonal antibody was from MitoSciences (Eugene, OR). RME1 and Dyn1 monoclonal antibodies were purchased from the Developmental Studies Hybridoma Bank (Japan). Na-$K^+$ATPase was from Upstate Biotechnology (Charlottesville, VA). Bip monoclonal antibody and caveolin polyclonal antibody were from BD Biosciences. Actin monoclonal antibody and Rab7 was from Santa Cruz Biotechnology (Santa Cruz, CA). Rab18 was from Calbiochem (San Diego, CA). Gelatin and tannic acid were from Sigma-Aldrich (Missouri, USA). Formvar was from BDH Chemicals. Ltd. (Poole, UK). Uranyl acetate, 25% glutaraldehyde solution (EM grade), and a low viscosity embedding media Spurr's Kit were all from Electron Microscopy Sciences (Hatfield, PA). Osmium tetraoxide (EM grade) was purchased from Nakalai Tesque Co. (Kyoto, Japan). Phosphotungstic acid was from Zhongjingkeyi Technology Co., Ltd. (Beijing, China).

*Strains and Culture Conditions*—The N2 Bristol strain and VS20 (pATGL-1::ATGL-1::GFP) were used in this study. Animal culture was conducted essentially the same as previously described (22). Briefly, *E. coli* strain OP50 was cultured in LB medium and seeded onto 9-cm and 15-cm Nematode Growth Medium plates. Synchronized L1 stage animals were then seeded onto the plates. Animal density was ~50 per $cm^2$. Animals were harvested for LD isolation at the young adult stage (24 h post L4 stage).

*Isolation of Lipid Droplets*—LDs were isolated using a modified method previously described (12). First, about $4 \times 10^5$ worms were harvested and washed three times with 50 ml PBS/0.001% Triton-X100. Worm pellets were then washed with 50 ml buffer A (25 mM Tricine, pH 7.6, 250 mM sucrose, and 0.2 mM phenylmethylsulfonyl fluoride), homogenized using a polytron (Cole-Parmer® Labgen™ 125 and 700 Tissue Homogenizers) in 10 ml buffer A, and centrifuged at 1000 $\times$ *g* for 30 s. The supernatant was homogenized again by nitrogen cavitation (Ashcroft Duralife Pressure Gauge) at 500 psi for 15 min on ice, and then centrifuged at 1000 $\times$ *g* for 10 min. Nine milliliters of this postnuclear supernatant (PNS) was loaded into an SW40 tube, and 3 ml buffer B (20 mM HEPES, pH 7.4, 100 mM KCl, and 2 mM $MgCl_2$) was overlaid on top. The tube was then centrifuged at 12,628 $\times$ *g* for 1 h at 4 °C. The LD fraction was carefully collected from the top layer and washed three times with 200 $\mu$l buffer B.

*Protein Preparation and Western Blotting*—Proteins were extracted and analyzed using Western blotting by a method described in our previous study (16).

*Mass Spectrometry Analysis*—The protocol used was the same as previously described (39). LD-proteins were subjected to reduce with 10 mM dithiotreitol by incubating at 56 °C for 1 h and then alkylated for 45 min by 55 mM iodoacetamide in the dark. Proteins were then incubated with 10 $\mu$l trypsin solution (10 ng/$\mu$l in 25 mM ammonium bicarbonate) for 30 min on ice. After removing excess enzyme solution, 30~40 $\mu$l 25 mM ammonium bicarbonate was added, and digestion was allowed to proceed at 37 °C overnight. Five percent formic acid was added to stop the digestion reaction, which was then vortexed and centrifuged. A $C_{18}$ trap column was used to add the peptide solution, eluted and then subjected to nano-LC-ESI-LTQ Orbitrap XL MS/MS analysis. The Orbitrap mass spectrometer was operated under data-dependent mode and was set at an initial 300~1800 Da MS scan range. All MS/MS data were searched against the WormBase database Wormpep218, which was released on August 22, 2010, and contains 24761 protein sequences. The BioWorks (3.31 sp1) Sequest search parameters were as follows: enzyme: trypsin; precursor ion mass tolerance: 2.0 Da; and fragment ion mass tolerance: 1.0 Da. The variable modification was set to oxidation of methionine (Met +15.99 Da). The fixed modification was set to carboxyamidomethylation of cysteine (Cys +57.02 Da). The search results were filtered with Xcorr *versus* Charge values of, Xcorr (+2) > 2.5, and Xcorr (+3) > 3.5. Two times peptide FDR: $FDR_1$ = 0.434%, $FDR_2$ = 0.426%. peptide mass accuracy < 5ppm, SP score > 500, RSp < 5. distinct peptides≥2, misscleavages 2.

*Transmission Electron Microscopy*—The purity of LDs was examined by transmission electron microscopy. Negative staining, whole mount EM, and ultra-thin sectioning methods were used. For negative staining, the sample of purified LDs was loaded onto a carbon-coated, Formvar-covered copper grid and stained for 1 min by 0.5% neutral phosphotungstic acid. To view the isolated LDs by whole mount EM, a carbon-coated, Formvar-covered copper grid was placed onto a drop of isolated LD suspension. The grid was then placed onto a drop of 2.5% glutaraldehyde solution (0.1 M PBS, pH 7.2) for 10 min and subsequently onto a drop of 2% osmium tetraoxide solution (0.1 M PBS, pH 7.2) for 10 min to fix the LDs. After fixation, LDs were stained with 0.1% tannic acid for 10 min and 2% uranyl acetate for 10 min. After each step, the grid was washed with deionized water three times, 1 min each time. For ultra-thin sectioning of purified LDs, the LD sample was first embedded in 10% gelatin (0.1 M PBS, pH 7.2). After solidification, the sample was cut into small blocks and prefixed in 2.5% glutaraldehyde (0.1 M PBS, pH 7.2) for 12 h at 4 °C and post-fixed in 2% osmium tetraoxide for 24 h at 4 °C. The sample was then dehydrated in an ascending series of ethanol concentrations at room temperature and embedded in Spurr. Sections of a thickness of 70 nm were prepared with a Leica EM UC6 Ultramicrotome (Leica Germany) and loaded onto Formvar-covered copper grids. Grids were then stained with 2% uranyl acetate for 15 min at room temperature before viewing with a FEI Tecnai 20 (FEI Co., Netherlands) electron microscope.

*Nile Red Staining of C. elegans*—Fixed Nile Red staining of *C. elegans* was performed as previously described (24). Approximately 200~1000 nematodes were suspended in 1 ml of water. Fifty microliters of freshly prepared 10% paraformaldehyde solution was added, mixed, and worms were rocked for 1 h at room temperature. Worms were allowed to settle, and then the paraformaldehyde solution was replaced by 1 ml of 1 $\mu$g/ml Nile Red in M9 and incubated for 15~30 min at room temperature, with occasional gentle agitation. After most of the staining solution was removed, the fixed worms were mounted onto 2% agarose pads for microscopic observation and photography.

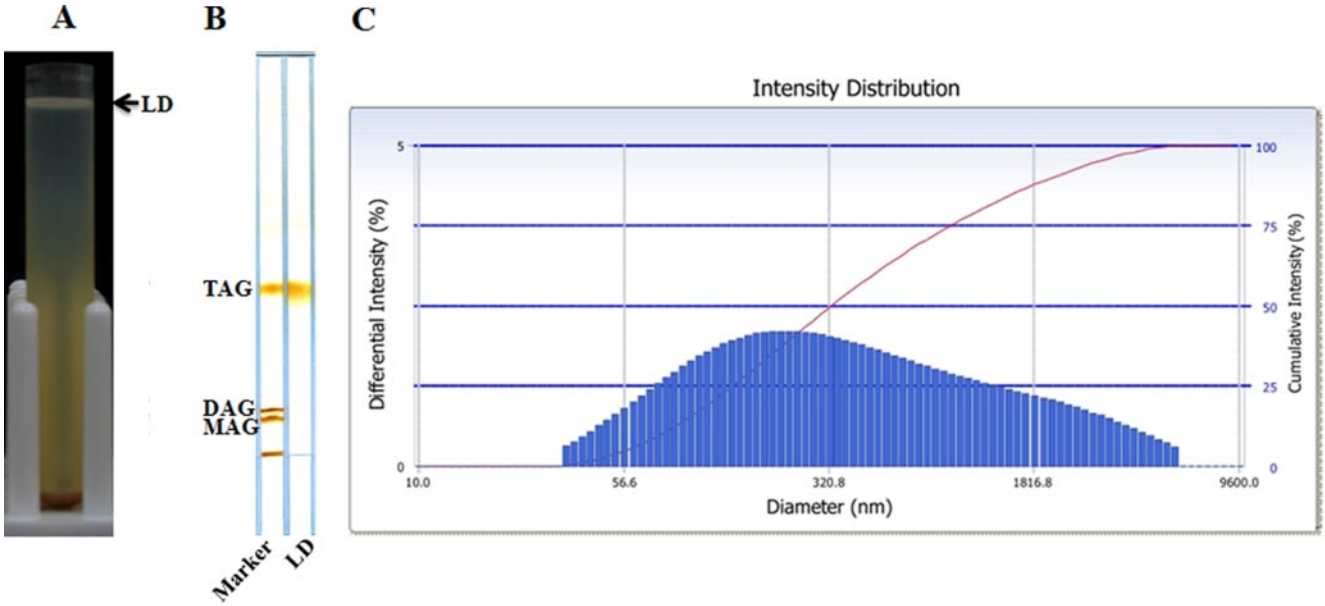


FIG. 1. **Isolation of lipid droplets from *C. elegans*.** *A*, $4 \times 10^5$ young adult wild-type *C. elegans* worms were harvested, washed, and homogenized. The PNS was centrifuged at 12,628 × *g* for 1 h. The top white layer was the lipid droplet (LD) fraction. *B*, Total lipids were extracted from the LD fraction with chloroform:acetone (1:1, v/v) and separated by thin layer chromatography (TLC) in a hexane:diethyl ether:acetic acid (80:20:1, v/v/v) solvent system. The LD fraction contained mainly TAG. *C*, The size of the purified LDs was measured by a Delsa Nano C particle analyzer. The diameters of LDs were in the range of 50 nm to 3000 nm.

*Confocal Microscopy*—Purified LDs were stained with Nile Red and viewed with an Olympus Fluoview1000 as described previously (39).

Confocal microscopy images of fixed worms were obtained using a Spinning Disk Confocal Microscope (Zeiss). The figures were produced using a 100 × 1.45 numerical aperture oil objective (Olympus PLAN APO) and an electron-multiplying charge-coupled device (EMCCD) camera (Andor iXon DV-897 BV). The fluorescence signals were analyzed by Image J software (NIH).

For photobleaching experiment, the worms were anesthetized in 0.01% tetramisole hydrochloride in PBS for 30 min and mounted on 2% agarose pads. We identified the area of interest on the Olympus Fluoview1000, brought it to the desired focus, defined a region of interest for the photobleach, and chose photobleaching conditions so that after photobleaching the fluorescent signal of the photobleached area decreases to background intensity levels. The bleaching conditions require a 100∼1000-fold increase in laser power for 20 bleach iterations (roughly 2 s) with 100% transmission of a 488 nm laser. After bleaching, the image of the selected area was captured every 2 min for 10 min.

*Thin Layer Chromatography (TLC)*—Lipids were extracted and analyzed using TLC by a method described in our previous study (17).

## RESULTS

*Isolation of Lipid Droplets from C. elegans*—Using our newly established method, we successfully isolated LD fraction in large quantity on top of a density gradient (Fig. 1*A*). The LD fraction was then washed three times to remove co-isolated cytosolic proteins and other cellular organelles. To test its lipid composition, we extracted total lipids from the LD fraction by chloroform and acetone, and then separated different lipid species by TLC. TLC results showed that triacylglycerol (TAG) was highly enriched in the fraction (Fig. 1*B*). We also measured the size of isolated LDs by a Delsa Nano C particle analyzer. As shown in Fig. 1C, the size of LDs was distributed in the range of 50 nm to 3,000 nm. All these characterizations such as density, lipid composition, and size were agreed with previous isolated lipid droplets from other sources (1, 17, 26, 27).

*Verification of the Purity of Isolated Lipid Droplets*—To further test the purity of isolated LDs, transmission electron microscopy (TEM) images were taken. The results showed that all the isolated LDs appeared as spherical structures and, importantly, that membrane debris and other cellular organelles were barely detected (Fig. 2*A*, *upper* panels). With Nile red staining and DIC imaging, purified LDs appeared to be a bead structure (Fig. 2*A*, *lower* panels), similar to purified LDs from CHO K2 cells (12, 17). We then analyzed the LD-protein profile using gel electrophoresis. The protein pattern of isolated LDs was significantly different from the other three cellular fractions (Fig. 2*B*). In addition, three independent isolations were analyzed and their protein profiles were almost identical, suggesting the reproducibility and quality of the purification method (supplemental Fig. S1). Immunoblotting was used to further verify the purity of the LDs (Fig. 2*C*). Equal amounts of proteins from LD, total membrane (TM), cytosol (Cyto), and PNS fractions were separated by SDS-PAGE and detected by the antibodies indicated. Fig. 2*C* shows clearly that the isolated LDs had little contamination with mitochondria (PDH-E1$\alpha$), endosomes (RME), ER (Bip), plasma membranes (Na-$K^+$ ATPase), cellular membranes (Dyn), or cytosol (actin). In the LD fraction we observed the enrichment of Rab 18 and Rab 7, proteins previously identified (12, 17) in LDs isolated from CHO cells (Fig. 2*C*).

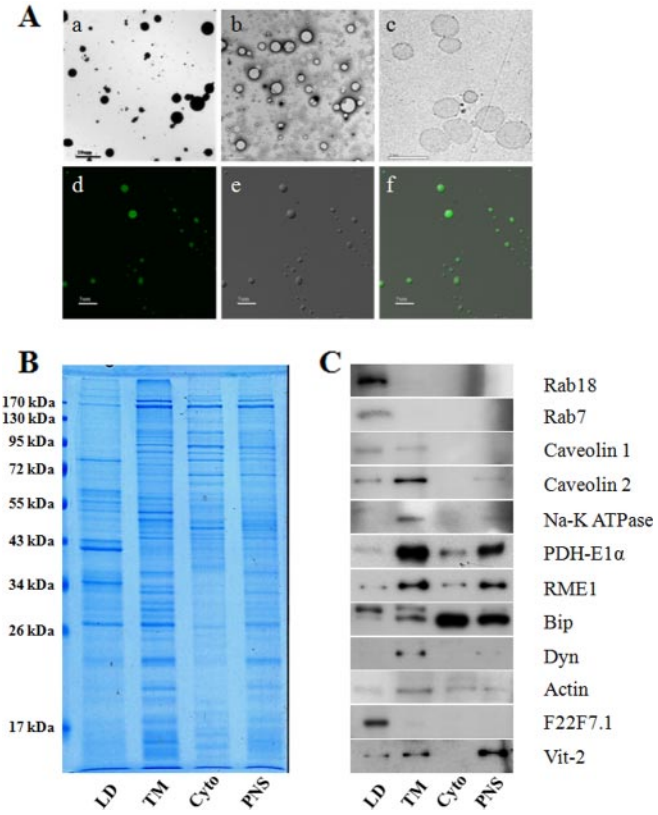


FIG. 2. **Verification of purified lipid droplets.** *A*, Isolated LDs were first analyzed by TEM with positive-staining (a), and negative-staining (b) and by ultra-thin sectioning (c), and then by light microscopy with Nile red staining (d) by DIC microscopy (e), and by merging images (f). *B*, Proteins extracted from isolated lipid droplet (LD), total membrane (TM), cytosol (Cyto), and PNS fractions were separated by SDS-PAGE and stained by Colloidal blue. Note the distinct banding pattern of LDs. *C*, The same protein samples were also subjected to Western blotting to test for contamination from other cellular fractions. Specific antibodies were used to probe for marker proteins of different cellular organelles/fractions; Rabs and caveolins (LD proteins), caveolins and Na-K ATPase (plasma membrane), PDH-E1$\alpha$ (mitochondrion), RME1 (endosome), Bip (endoplasmic reticulum), Dyn (membrane), actin (cytosol), F22F7.1 and Vit-2 (lipid droplet-associated proteins).

*Proteomic and Bioinformatic Analyses of Lipid Droplet Proteins*—Having verified the purity of isolated LDs by biochemical and morphological examinations, we extracted proteins from the purified LDs and subjected them to nano-LC-ESI-LTQ Orbitrap XL MS/MS analysis. From two independent proteomic studies, we identified 306 proteins that were presented in both analyses (Table I and Fig. 3*A*), and Table S1 shows the top 50 abundant proteins. It was found that 63% of these proteins had been identified in previous LD proteomic studies (Fig. 3*B*). When this proteome was compared with one previous proteomic study that was done using Chinese hamster ovary cells (CHO K2) (16), 28 of 125 LD proteins of CHO cells were overlapped with LD-associated proteins from *C. elegans* (Fig. 3*C*). We classified these proteins into nine groups by function or localization: lipid metabolism, other metabolism, transcription, ribosome, membrane trafficking, chaperone, signal transduction, cytoskeleton, and proteins with unknown function (Fig. *3D)*. The enrichment (41%) of proteins involved in metabolism further indicates the similarity of *C. elegans* LDs to other eukaryotic LDs.

To determine the relationships between these 306 proteins, we analyzed our data with STRING 9.0 using default parameters (28). supplemental Fig. S2 summarizes the network of predicted associations for these proteins. Some of these proteins showed close relationships and formed two main clusters. The densest cluster (upper cluster) consists of 53 ribosome proteins. Identification of ribosome proteins on LDs has also been reported in some early LD proteomic studies in humans (12), yeast (10), and *Drosophila* (18). This finding suggests that LDs may provide a surface for ribosomes where certain proteins can be efficiently synthesized. The other cluster (lower cluster) mainly consists of metabolic proteins that are involved in processes such as lipid metabolism, energy generation, and nucleotide biosynthesis. These results are consistent with early reports that LDs are not only centers for lipid synthesis, storage and metabolism, but also provide extra membrane surface area for protein synthesis and intracellular reactions.

*Identification of DHS-3 as a C. elegans Lipid Droplet Marker Protein*—Because dehydrogenases are found in most of previous LD proteomes, we constructed a transgenic line that expresses the fusion protein DHS-3::GFP under the control of a *daf-22* promoter in gut epithelial cells. Interestingly, DHS-3::GFP formed ring structures *in vivo*, typical of the localization pattern of PLIN proteins (Fig. 4*A*). To validate this result biochemically, we probed the distribution of the DHS-3::GFP protein in the transgenic line using a GFP antibody and an anti-DHS-3 antibody that was generated in our lab. The Western blotting result (Fig. 4*B*) shows that the two antibodies recognized a single band of molecular weight ~63 kDa, verifying the specificity of the DHS-3 antibody and GFP-fusion protein expression. Using the DHS-3 antibody, we detected DHS-3 in the purified LD fraction but not in the total membrane (TM), cytosol (Cyto), or PNS fractions of wild-type *C. elegans* with equal protein loading (Fig. 4*C*). To further analyze the enrichment of DHS-3 in the LD fraction, we tested an excess of the PNS fraction (10 $\times$ and 50$\times$) using the DHS-3 antibody (Fig. 4*D*). A very weak DHS-3 signal was detected in the PNS fraction at 10-fold excess loading (Fig. 4*D*). Although 50-fold excess protein loading, the DHS-3 signal of PNS fraction was still much lower than the signal of LD (Fig. 4*D*). In addition, to determine if DHS-3 is a dynamic protein on LDs, selected regions of the worm were photobleached and then the fluorescent signal in those regions was detected in every 2 min, up to 10 min after bleaching (Fig. 4*E*). Recovery of fluorescent signals was not observed, indicating that neither DHS-3 was recruited to the bleached LDs from other cellular compartments (arrow-pointed regions) nor translocated to the bleached part from non-bleached part of

TABLE I
*C. elegans Lipid Droplet-associated Proteins*

| Sequence name | Protein ID | Gene name | Citations | Sequence name | Protein ID | Gene name | Citations |
|---|---|---|---|---|---|---|---|
| Lipid Metabolism | | | | | | | |
| E04F6.5a | CE01217 | acdh-12 | (16) | T05F1.10 | CE26900 | dhs-4 | (16, 40) |
| F49H12.6a | CE23754 | acl-4 | (39) | Y32H12A.3 | CE21514 | dhs-9 | (16) |
| Y65B4BL.5 | CE24550 | acs-13 | (13, 41) | C29F3.1 | CE08435 | ech-1 | |
| C46F4.2 | CE30907 | acs-17 | (10, 13, 41) | Y56A3A.12a | CE24467 | faah-4 | (19) |
| F37C12.7 | CE29312 | acs-4 | (13, 41) | ZK973.10 | CE40009 | lpd-5 | |
| Y76A2B.3 | CE19275 | acs-5 | (13, 41) | Y66H1B.4 | CE20348 | spl-1 | |
| T11F9.11 | CE06423 | dhs-19 | | T25G3.4 | CE14180 | | (16) |
| T02E1.5a | CE41004 | dhs-3 | | Y53G8B.2 | CE25428 | | (19) |
| Other Metabolism | | | | | | | |
| F40F9.6a | CE05855 | aagr-3 | | K12G11.3 | CE12212 | sodh-1 | (16, 40) |
| Y50D7A.7 | CE26144 | ads-1 | | Y47G6A.10 | CE34400 | spg-7 | (11, 16) |
| T05H4.13a | CE27441 | alh-4 | (16) | F23H12.2 | CE05705 | tomm-20 | |
| F13D12.4a | CE02183 | alh-8 | (15) | F56D2.1 | CE11226 | ucr-1 | (41, 42) |
| T27E9.1a | CE14263 | ant-1.1 | (19) | VW06B3R.1a | CE20123 | ucr-2.1 | (41, 42) |
| W02D3.6 | CE14428 | ant-1.2 | (19) | T10B10.2 | CE23962 | ucr-2.2 | (41, 42) |
| K01H12.2 | CE03454 | ant-1.3 | (19) | T24C4.1 | CE19592 | ucr-2.3 | (16, 41, 42) |
| T01B11.4 | CE12898 | ant-1.4 | (19) | Y38F2AL.3a | CE29997 | vha-11 | (11, 13, 16, 43) |
| F08C6.6 | CE27925 | apy-1 | | Y49A3A.2 | CE22210 | vha-13 | (11, 13, 16, 43) |
| F01G4.2 | CE03127 | ard-1 | (16, 40, 43) | T14F9.1 | CE07497 | vha-15 | (11, 13, 16, 43) |
| F35G12.10 | CE00968 | asb-1 | (13, 43) | M03C11.5 | CE43540 | ymel-1 | |
| F02E8.1 | CE07016 | asb-2 | (11, 13, 43) | T26C12.1 | CE26009 | | |
| K07A12.3 | CE11868 | asg-1 | (13, 43) | B0303.3 | CE00561 | | (15) |
| C53B7.4 | CE06974 | asg-2 | (13, 43) | T22B11.5 | CE28486 | | (16) |
| R12H7.2 | CE03567 | asp-4 | | T08B2.7a | CE13431 | | (16) |
| F54B3.3 | CE35878 | atad-3 | (11, 16) | F09E5.2 | CE32364 | | |
| C34E10.6 | CE29950 | atp-2 | (13, 43) | H28O16.1a | CE18826 | | (13, 43) |
| F27C1.7a | CE09719 | atp-3 | (11, 16) | F58F12.1 | CE01976 | | (13, 43) |
| T05H4.12 | CE13291 | atp-4 | (13, 43) | R53.4 | CE03574 | | (13, 43) |
| C06H2.1 | CE15602 | atp-5 | (13, 43) | F32D1.2 | CE09866 | | (13, 43) |
| T06D8.6 | CE02327 | cchl-1 | | W10C8.5 | CE18353 | | |
| Y37D8A.14 | CE20218 | cco-2 | | LLC1.3a | CE31971 | | (16) |
| K01D12.12 | CE06051 | cdr-6 | | ZK829.4 | CE06652 | | (16) |
| R07H5.2a | CE18907 | cpt-2 | (12) | T22D1.4 | CE33704 | | |
| C54G4.8 | CE05514 | cyc-1 | (18, 42) | F48E3.3 | CE02751 | | |
| W02D3.2 | CE14420 | dhod-1 | (16) | F59C6.5 | CE11464 | | (15) |
| F46E10.9 | CE20819 | dpy-11 | | D2030.4 | CE09081 | | (16) |
| B0365.3 | CE07721 | eat-6 | (11, 16) | T05H4.5 | CE13277 | | (15, 41, 42) |
| K09A9.5 | CE11980 | gas-1 | (15) | F53F4.10 | CE10972 | | (15, 41, 44) |
| T14G11.3 | CE33696 | immt-1 | | C33A12.1 | CE05347 | | (15) |
| W06H3.1 | CE36215 | immt-2 | | C16A3.5 | CE04005 | | (15) |
| F42G8.12 | CE17071 | isp-1 | (18, 41, 42) | F37C4.6 | CE17049 | | |
| C05D11.12 | CE29662 | let-721 | (45) | T05H10.6a | CE01643 | | (11, 16) |
| Y22F5A.4 | CE16605 | lys-1 | | F47B10.1 | CE03351 | | |
| B0546.1 | CE16792 | mai-2 | (16) | T02H6.11 | CE21147 | | (16, 41, 42) |
| F20H11.3 | CE09512 | mdh-1 | (16) | Y53G8AL.2 | CE26163 | | |
| T26A5.3 | CE00702 | nduf-2.2 | (15) | Y69A2AR.18a | CE27514 | | |
| Y54E10BL.5 | CE22460 | nduf-5 | (15) | Y51H1A.3a | CE20284 | | |
| F22D6.4 | CE05685 | nduf-6 | (15) | B0491.5 | CE02107 | | |
| W10D5.2 | CE14780 | nduf-7 | (15) | W09C5.8 | CE20171 | | |
| C09H10.3 | CE02132 | nuo-1 | (15) | Y71H2AM.5 | CE22939 | | |
| T10E9.7a | CE37406 | nuo-2 | (15) | C34B2.8 | CE16896 | | |
| Y57G11C.12b | CE14948 | nuo-3 | (15) | R04F11.2 | CE06233 | | |
| K04G7.4a | CE01361 | nuo-4 | (15, 44) | C25H3.9a | CE44829 | | |
| Y45G12B.1a | CE21933 | nuo-5 | (15) | C27D8.4 | CE30618 | | |
| T09A5.11 | CE01081 | ostb-1 | | F45H10.2 | CE10544 | | |
| F27D9.5 | CE04451 | pcca-1 | (42) | R07E4.3 | CE04818 | | |
| F52E4.1a | CE07269 | pccb-1 | (42) | Y53F4B.18 | CE22408 | | |
| K11D9.2a | CE18884 | sca-1 | (11, 16) | F52H2.6 | CE10874 | | |
| C01F1.2 | CE06743 | sco-1 | | ZK550.3 | CE37464 | | |

TABLE I—*continued*

| Sequence name | Protein ID | Gene name | Citations | Sequence name | Protein ID | Gene name | Citations |
|---|---|---|---|---|---|---|---|
| C03G5.1 | CE03917 | sdha-1 | (16) | F23B12.5 | CE09597 | | |
| C34B2.7 | CE16895 | sdha-2 | (16) | Y47D3B.10 | CE20261 | | |
| F42A8.2 | CE01579 | sdhb-1 | (16) | MTCE.11 | CE34065 | | |
| C54H2.5 | CE06987 | sft-4 | | F45H10.3 | CE10546 | | |
| Trafficking and Transport | | | | | | | |
| F44B9.5 | CE24973 | aup | (41, 42, 44) | Y66D12A.22 | CE28800 | tin-10 | |
| M03F4.7a | CE12368 | calu-1 | | C18E9.6 | CE05298 | tomm-40 | |
| Y38A10A.5 | CE21562 | crt-1 | | F53F10.4 | CE10986 | unc-108 | (40) |
| D2013.5 | CE42493 | eat-3 | (42) | K09F5.2 | CE04746 | vit-1 | (11, 39) |
| B0432.4 | CE32102 | misc-1 | | C42D8.2a | CE06950 | vit-2 | (11, 39) |
| C17E4.9 | CE08258 | nkb-1 | (11, 16) | F59D8.1 | CE20900 | vit-3 | (11, 39) |
| C02E11.1a | CE28528 | nra-4 | | F59D8.2 | CE26817 | vit-4 | (11, 39) |
| M117.2 | CE06200 | par-5 | | C04F6.1 | CE03921 | vit-5 | (11, 39) |
| C39F7.4 | CE16905 | rab-1 | (15, 40) | K07H8.6a | CE28594 | vit-6 | (11, 39) |
| F53G12.1 | CE11006 | rab-11.1 | (40) | T08G11.1a | CE13443 | | |
| Y92C3B.3b | CE27340 | rab-18 | (13, 41) | R05G6.7 | CE29443 | | (43) |
| W03C9.3 | CE03777 | rab-7 | (13, 40–42) | F01G4.6a | CE09162 | | |
| D1037.4 | CE30373 | rab-8 | (40) | Y7A5A.1 | CE21326 | | |
| Y51H4A.3 | CE25369 | rho-1 | (16, 40) | T20H4.5 | CE00832 | | |
| W06H8.1a | CE25146 | rme-1 | | T10F2.2 | CE02041 | | |
| T21C9.12 | CE06481 | scpl-4 | (19) | W02D3.1 | CE14418 | | (18, 41, 42) |
| W08E3.3 | CE14708 | tag-210 | (42) | K11H3.3 | CE00474 | | |
| Chaperone | | | | | | | |
| C47E8.5 | CE05441 | daf-21 | (41, 44) | H06O01.1 | CE11570 | pdi-3 | (15, 41, 44) |
| F26D10.3 | CE09682 | hsp-1 | (41, 44) | Y37E3.9 | CE26775 | phb-1 | (12, 13, 16) |
| C15H9.6 | CE08177 | hsp-3 | (41, 44) | T24H7.1 | CE40718 | phb-2 | (12, 13, 16) |
| F43E2.8 | CE07244 | hsp-4 | (41, 44) | F43D9.4 | CE00994 | sip-1 | (41, 44) |
| Y22D7AL.5b | CE42184 | hsp-60 | (39, 41, 44) | B0403.4 | CE03880 | tag-320 | (15, 41, 44) |
| C14B1.1 | CE00897 | pdi-1 | (15, 41, 44) | T05E11.3 | CE06362 | | (40) |
| C07A12.4a | CE03972 | pdi-2 | (15, 41, 44) | | | | |
| Cytoskeleton | | | | | | | |
| T04C12.6 | CE13148 | act-1 | (40) | ZK154.3 | CE15257 | mec-7 | (13, 40) |
| T04C12.5 | CE13150 | act-2 | (40) | F26E4.8 | CE09692 | tba-1 | (13, 40) |
| T04C12.4 | CE13148 | act-3 | (40) | C47B2.3 | CE17563 | tba-2 | (13, 40) |
| M03F4.2a | CE12358 | act-4 | (40) | F44F4.11 | CE18680 | tba-4 | (13, 40) |
| T25C8.2 | CE16463 | act-5 | (40) | T28D6.2 | CE16521 | tba-7 | (13, 40) |
| C54C6.2 | CE33770 | ben-1 | (13, 40) | K01G5.7 | CE16197 | tbb-1 | (13, 40) |
| W09H1.6a | CE16576 | lec-1 | | C36E8.5 | CE00913 | tbb-2 | (13, 40) |
| ZC8.4a | CE31264 | lfi-1 | | B0272.1 | CE00850 | tbb-4 | (13, 40) |
| Signal Transduction | | | | | | | |
| T20G5.1 | CE00480 | chc-1 | (16) | W10D9.5 | CE14794 | tomm-22 | |
| ZK632.6 | CE00423 | cnx-1 | (13, 44) | Y56A3A.32 | CE31841 | wah-1 | |
| F40E10.3 | CE05839 | csq-1 | | ZK856.8 | CE06665 | | |
| F52H3.7a | CE32894 | lec-2 | | Y54G2A.2a | CE26776 | | |
| F58G11.1a | CE11400 | letm-1 | | Y54G2A.18 | CE25462 | | |
| K04D7.1 | CE06090 | rack-1 | | K01G5.5 | CE16195 | | |
| Transcription | | | | | | | |
| F31E3.5 | CE01270 | eef-1A.1 | (16, 19) | B0035.9 | CE03252 | his-46 | (19, 42) |
| R03G5.1a | CE01270 | eef-1A.2 | (16, 19) | F07B7.9 | CE03252 | his-50 | (19, 42) |
| F25H5.4 | CE15900 | eef-2 | (16, 19) | F54E12.3 | CE03252 | his-56 | (19, 42) |
| T01C3.7 | CE12920 | fib-1 | | F55G1.11 | CE03252 | his-60 | (19, 42) |
| F45F2.12 | CE10538 | his-8 | (19, 42) | F22B3.1 | CE03252 | his-64 | (19, 42) |
| K06C4.10 | CE03252 | his-18 | (19, 42) | K07A1.8 | CE11854 | ile-1 | |
| K06C4.2 | CE03252 | his-28 | (19, 42) | F57B9.6a | CE01341 | inf-1 | |
| F17E9.12 | CE03252 | his-31 | (19, 42) | R74.1 | CE16317 | lars-1 | |
| C50F4.7 | CE03252 | his-37 | (19, 42) | W01A8.1b | CE06531 | mdt-28 | |
| K03A1.6 | CE03252 | his-38 | (19, 42) | F10G7.2 | CE02626 | tsn-1 | |
| Ribosome | | | | | | | |
| F25H2.10 | CE09655 | rla-0 | (19, 46) | R13A5.8 | CE01380 | rpl-9 | (19, 46) |
| Y37E3.7 | CE26658 | rla-1 | (19, 46) | B0393.1 | CE00854 | rps-0 | (19, 46) |
| Y62E10A.1 | CE22694 | rla-2 | (19, 46) | F56F3.5 | CE00664 | rps-1 | (19, 46) |

TABLE I—*continued*

| Sequence name | Protein ID | Gene name | Citations | Sequence name | Protein ID | Gene name | Citations |
|---|---|---|---|---|---|---|---|
| Y71F9AL.13a | CE25552 | rpl-1 | (19, 46) | D1007.6 | CE09041 | rps-10 | (19, 46) |
| F10B5.1 | CE01543 | rpl-10 | (19, 46) | F40F11.1 | CE05860 | rps-11 | (19, 46) |
| T22F3.4 | CE13968 | rpl-11.1 | (19, 46) | F54E7.2 | CE26896 | rps-12 | (19, 46) |
| F07D10.1 | CE07033 | rpl-11.2 | (19, 46) | C16A3.9 | CE04009 | rps-13 | (19, 46) |
| JC8.3a | CE17986 | rpl-12 | (19, 46) | F37C12.9 | CE00821 | rps-14 | (19, 46) |
| C32E8.2a | CE08526 | rpl-13 | (19, 46) | F36A2.6 | CE09945 | rps-15 | (19, 46) |
| K11H12.2 | CE12148 | rpl-15 | (19, 46) | T01C3.6 | CE12918 | rps-16 | (19, 46) |
| Y48G8AL.8a | CE22195 | rpl-17 | (19, 46) | T08B2.10 | CE26948 | rps-17 | (19, 46) |
| Y45F10D.12 | CE16650 | rpl-18 | (19, 46) | Y57G11C.16 | CE14956 | rps-18 | (19, 46) |
| C09D4.5 | CE08034 | rpl-19 | (19, 46) | T05F1.3 | CE13265 | rps-19 | (19, 46) |
| B0250.1 | CE18478 | rpl-2 | (19, 46) | C49H3.11 | CE04237 | rps-2 | (19, 46) |
| C14B9.7 | CE00078 | rpl-21 | (19, 46) | F53A3.3a | CE10884 | rps-22 | (19, 46) |
| B0336.10 | CE00778 | rpl-23 | (19, 46) | K02B2.5 | CE04691 | rps-25 | (19, 46) |
| C53H9.1 | CE19381 | rpl-27 | (19, 46) | Y41D4B.5 | CE21842 | rps-28 | (19, 46) |
| F13B10.2a | CE05598 | rpl-3 | (19, 46) | C23G10.3 | CE01810 | rps-3 | (19, 46) |
| Y106G6H.3 | CE44850 | rpl-30 | (19, 46) | C26F1.4 | CE06878 | rps-30 | (19, 46) |
| W09C5.6a | CE20168 | rpl-31 | (19, 46) | Y43B11AR.4 | CE24278 | rps-4 | (19, 46) |
| T24B8.1a | CE03709 | rpl-32 | (19, 46) | T05E11.1 | CE06360 | rps-5 | (19, 46) |
| ZK652.4 | CE00450 | rpl-35 | (19, 46) | Y71A12B.1 | CE24592 | rps-6 | (19, 46) |
| F37C12.4 | CE30781 | rpl-36 | (19, 46) | ZC434.2 | CE06577 | rps-7 | (19, 46) |
| B0041.4 | CE07669 | rpl-4 | (19, 46) | F42C5.8 | CE04561 | rps-8 | (19, 46) |
| F54C9.5 | CE02255 | rpl-5 | (19, 46) | K07C5.4 | CE06114 | Ribosome | (19, 46) |
| F53G12.10 | CE11024 | rpl-7 | (19, 46) | C37A2.7 | CE30433 | Ribosome | (19, 46) |
| Y24D9A.4a | CE27398 | rpl-7A | (19, 46) | | | | |
| Unknown | | | | | | | |
| M176.3 | CE12464 | chch-3 | | F42G8.10a | CE17069 | | |
| K02F3.10 | CE01346 | moma-1 | | F54A3.5 | CE25901 | | |
| F30A10.5 | CE32397 | stl-1 | | W04C9.2 | CE18333 | | |
| Y56A3A.21 | CE22589 | trap-4 | | B0513.5 | CE37309 | | |
| K03H1.4 | CE00475 | ttr-2 | | Y57A10A.23 | CE22626 | | |
| Y51A2D.10 | CE19206 | ttr-25 | | Y54F10AM.5 | CE34127 | | |
| T28B4.3 | CE14325 | ttr-6 | | Y111B2A.2 | CE26622 | | |
| C31E10.7 | CE37487 | | | F29C4.2 | CE17720 | | |
| Y39B6A.10 | CE21698 | | | ZK809.3 | CE03831 | | |
| C25A1.12 | CE41871 | | | R53.5 | CE03575 | | |
| F22F7.1a | CE17691 | | | Y57G7A.10a | CE19639 | | |
| Y67H2A.5 | CE28376 | | | F49H12.5 | CE20835 | | |
| C10G11.7 | CE08086 | | | ZK1055.7 | CE18476 | | |
| F36A2.7 | CE09946 | | | K02F3.2 | CE39385 | | |
| F43E2.7a | CE41652 | | | Y92H12BR.3a | CE29936 | | |
| F32A11.1 | CE17737 | | | F59D6.7 | CE11488 | | |
| F44E5.1 | CE18676 | | | C41G7.9a | CE42828 | | |

the same LD (arrowhead-pointed region). After 20 min DHS-3::GFP signal was still not detected in the bleached region (supplemental Fig. S3). The notable position shift of LDs indicates that these LDs were still active during these 20 min. These results demonstrate that DHS-3 can be used as a protein marker for *C. elegans* LDs.

*Verification of Lipid Droplet Proteins*—To further confirm DHS-3 as a LD resident protein, we then constructed a transgenic line expressing the fusion protein pDHS-3::DHS-3::GFP under the control of its own promoter and observed that similar to pDAF22::DHS-3::GFP, pDHS-3::DHS-3::GFP also formed ring structures *in vivo* (Fig. 5*A*). To determine that these ring structures were LDs, purified LDs from DHS-3::GFP strain were analyzed using fluorescence and DIC microscopy (Fig. 5*B*). Almost all purified LDs detected by DIC were overlapped with fluorescence images. A few of DIC-detected LDs were not surrounded by GFP signals (Fig. 5*B*b, arrows), suggesting that not all LDs contain DHS-3. In addition, LDs in DHS-3::GFP strain were labeled using Nile Red fixed staining and merged with DHS-3::GFP fluorescence signals (Fig. 5*C*). Most Nile Red signals were surrounded with DHS-3::GFP (Fig. 5*C*c). These experiments proved that DHS-3::GFP ring structures are LDs.

More experiments were carried out to verify this LD proteomic study in *C. elegans*. Because ATGL was previously found in LDs of mammalian cells (12) and *C. elegans* (21, 29), it was chosen to do so. First, ATGL was indeed identified in the proteomics (Table I). Second, fluorescence study represented that pATGL::ATGL::GFP was colocalized with LDs stained by Lipid Tox (Fig. 5*D*). In addition, an unknown function protein F22F7.1

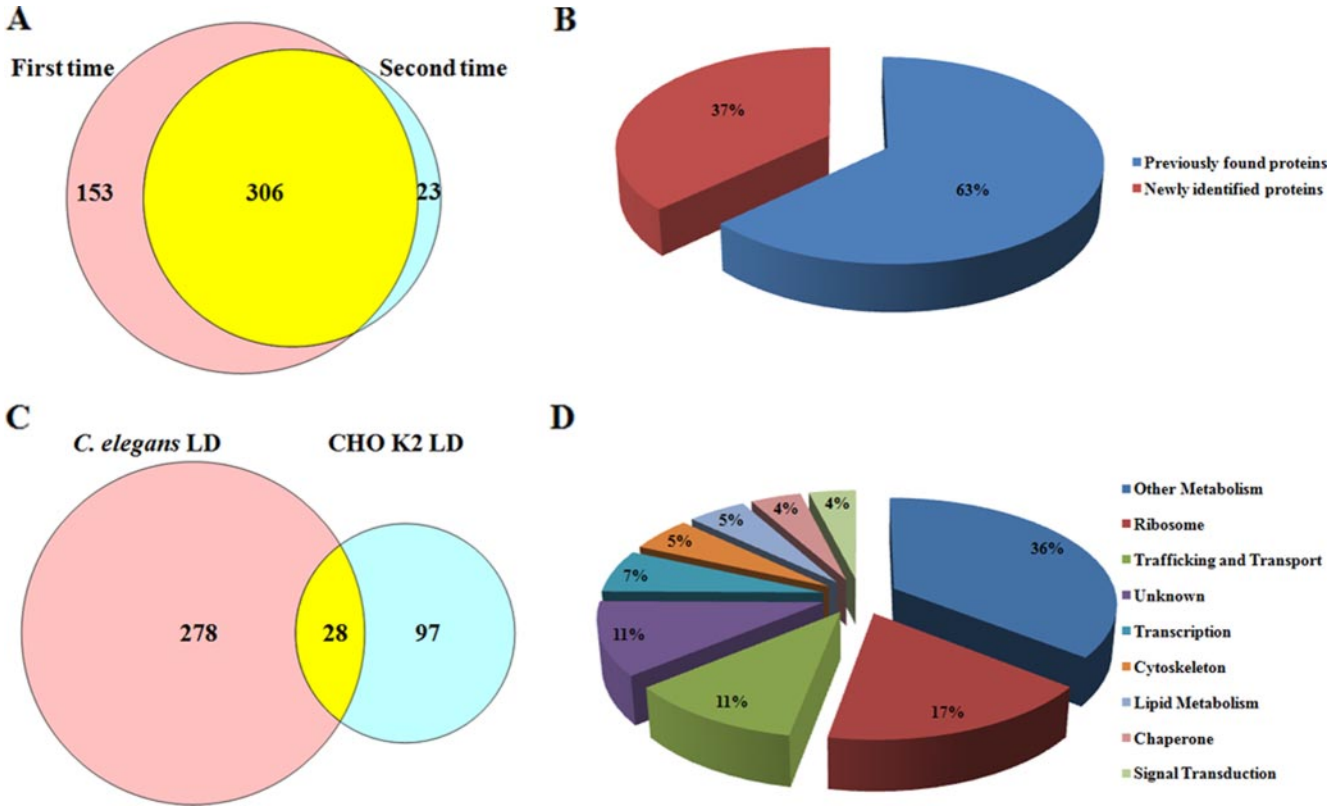


FIG. 3. **Proteomic and bioinformatic analyses of lipid droplet proteins.** *A*, LD proteins were precipitated by acetone and digested by trypsin then subjected to nano-LC-ESI-LTQ Orbitrap XL MS/MS analysis. The Venn Diagram showed the overlap of two independent mass spectrum results. *B*, LD proteins identified by mass spectrum were categorized to previously found proteins and newly identified proteins. *C*, The Venn Diagram showed the LD proteins identified in both *C. elegans* and Chinese hamster ovary K2 (CHO K2) cells. *D*, The 306 identified LD proteins were classified into 9 groups: lipid metabolism, other metabolism, transcription, ribosome, membrane traffic, chaperone, signal transduction, cytoskeleton, and unknown function.

and an apolipoprotein Vit-2 that were also identified by the proteomics were further verified. Western blotting experiments also showed that F22F7.1 was very enriched in LDs and Vit-2 was partially associated with LDs (Fig. 2*C*).

## DISCUSSION

We reported the purification and proteomic characterization of *C. elegans* LDs. Because of lack of LD marker proteins in *C. elegans*, we had to test the purity of our LD preparations by several other approaches. First, we demonstrated that the LD preparation was floated on top of gradient and highly enriched in TAG but not other lipid species. Second, our EM results showed that isolated LDs contained minimal contamination of other cellular organelles. Third, the protein pattern of LDs in SDS-PAGE was markedly different with TM, Cyto, and PNS. Fourth, using antibodies to detect specific marker proteins for each fraction, we detected only minimal mitochondrial, endosomal, ER, plasma membrane, and cytosolic contamination. Taken together, our results indicate that our LD preparations were relatively pure and suitable for proteomic analysis.

Results from our proteomics study suggest that *C. elegans* LDs and other eukaryotic LDs are conserved in that they share a large number of homologous proteins involved in lipid metabolism, membrane trafficking, and signal transduction. Of particular interest are the acyl-CoA synthetase (ACS) family, the homologue of mammalian adipose triglyceride lipase ATGL-1, and the short chain fatty acid dehydrogenases (DHS) family. *C. elegans* ACS-20 and ACS-22 are implicated in the incorporation of very long chain fatty acids into sphingomyelin, which may be linked to cuticle barrier formation (30). DHS-28, a peroxisomal dehydrogenase, has been shown to regulate long chain fatty acid $\beta$-oxidation and LD size (21). These proteins have also been identified in the LD proteome of other species (Table I). Another interesting category of LD-proteins shared between *C. elegans* and other species is proteins involved in trafficking and transport. We identified Rab1, 7, 8, 10, 11, and 18 in the *C. elegans* LD proteome. The small GTPase Rab18 localizes to LDs and promotes their close apposition to rough ER in human and mouse cells (2, 31). Rab10 and Rab35 have been shown to positively regulate LD size in *Drosophila S2* cells (32). Vit-1, 2, 3, 4, 5, and 6 were also present (Table I). Vit proteins are apolipoprotein homologs believed to transport lipids to growing oocytes during yolk deposition (33). Western blotting analysis showed that

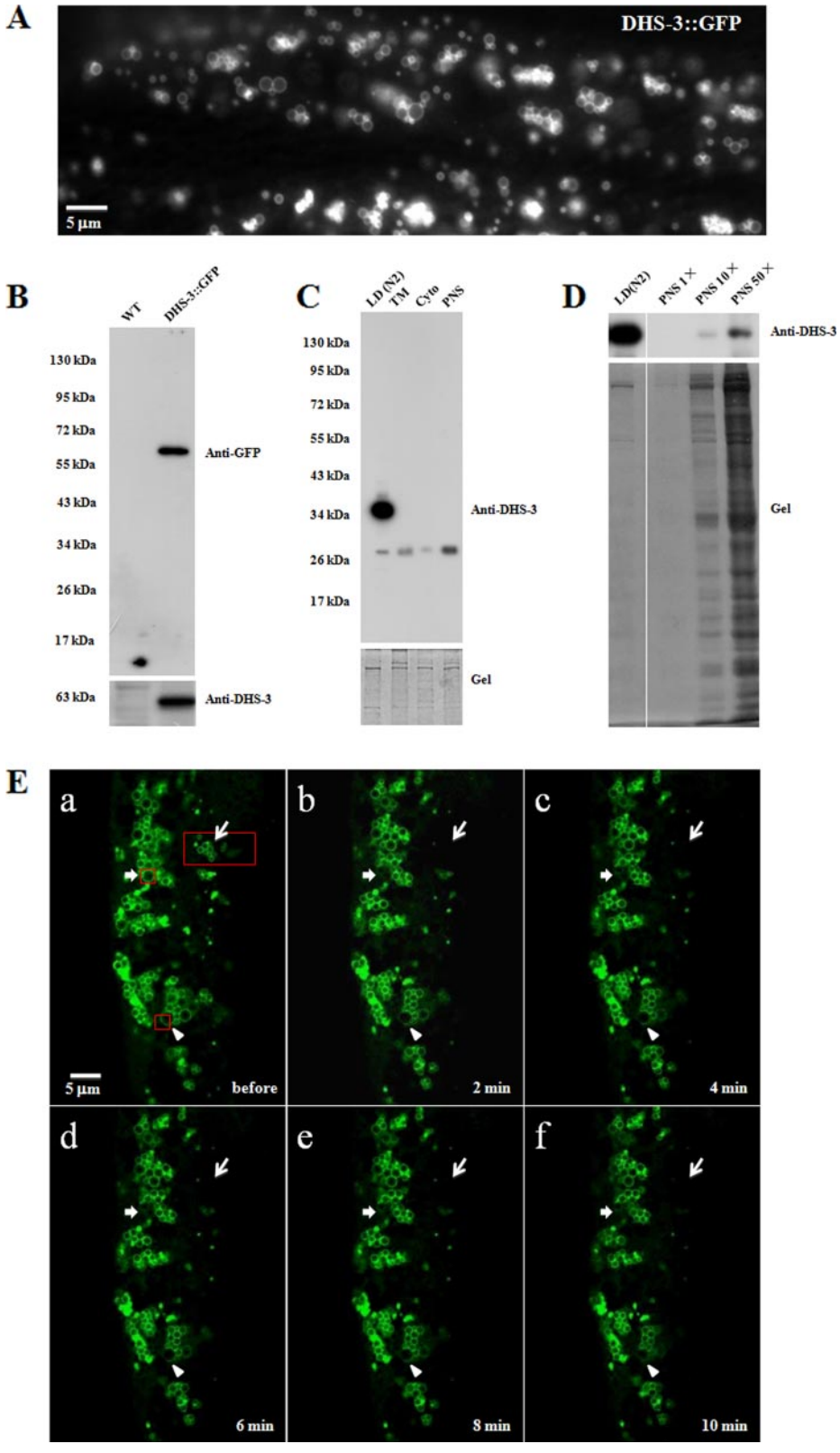


FIG. 4. **Identification of DHS-3 as a lipid droplet marker protein.** *A*, A DHS-3::GFP strain was used to observe the localization of DHS-3 using fluorescence microscopy. *B*, Western blotting of the WT and DHS-3::GFP strains using GFP (*upper* panel) and DHS-3 (*lower* panel) antibodies. *C*, Western blotting results confirmed that DHS-3 is mainly localized on LDs (*upper* panel). The original gel showing equal protein loading (*lower* panel). *D*, DHS-3 in LDs was dramatically enriched compared with the PNS (*upper* panel). The original gel (*lower* panel). *E*, The DHS-3::GFP strain was observed by fluorescence microscopy before photobleaching (a), after photobleaching (b/2 min, c/4 min, d/6 min, e/8 min, and f/10 min). The red boxes were the selected photobleaching regions: aggregated LDs (thin arrow), single LD (thick arrow), and partial LD (arrowhead).

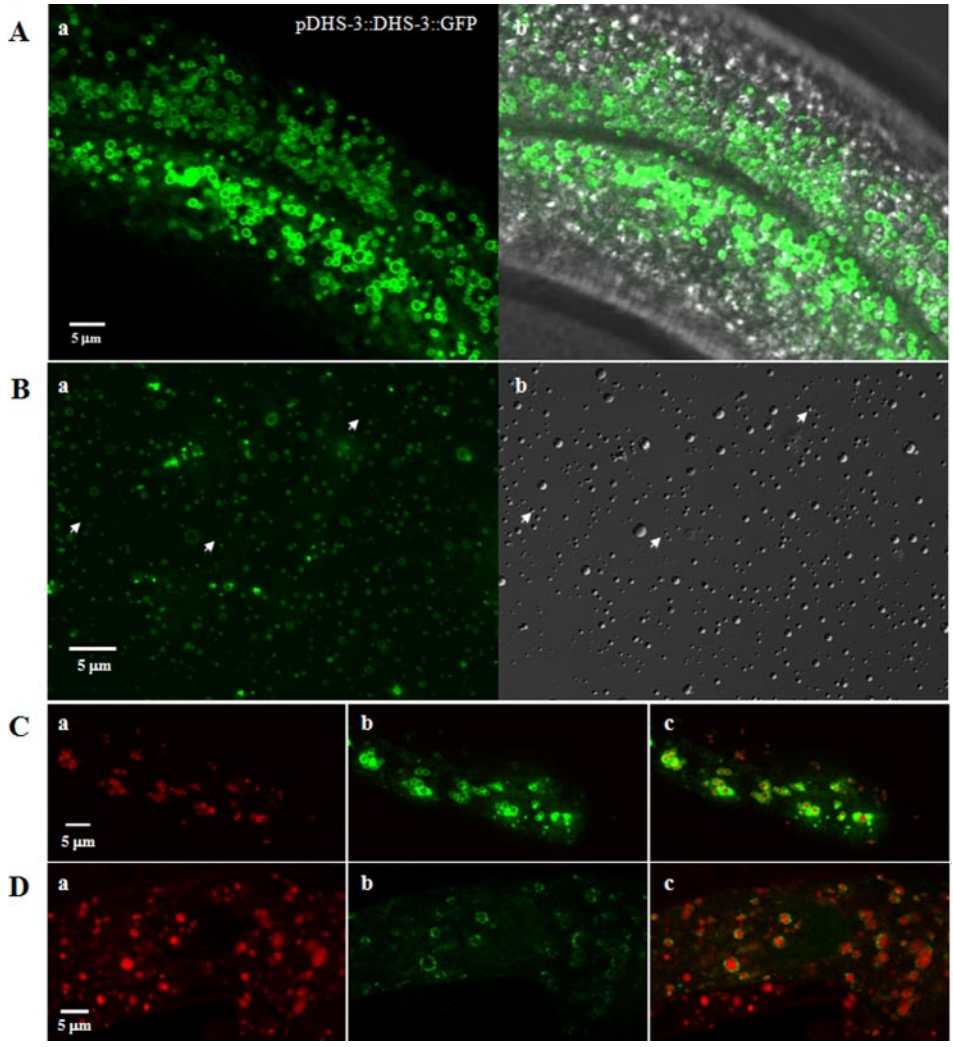


FIG. 5. **Verification of lipid droplet proteins.** *A*, A pDHS-3::DHS-3::GFP strain was used to observe the localization of endogenous DHS-3 using fluorescence microscopy (a) and merged with bright field. (b). *B*, Purified DHS-3::GFP lipid droplets were observed by fluorescence microscopy (a) and by DIC microscopy (b). *C*, Nile Red fixed staining of *C. elegans* in DHS-3::GFP strain. The fluorescence of fixed Nile Red (a), the fluorescence of DHS-3::GFP (b) and the merge of these two images (c). *D*, Lipid Tox deep Red staining of pATGL-1::ATGL-1::GFP strain (VS20). The fluorescence of Lipid Tox deep Red (a), the fluorescence of ATGL-1::GFP (b) and the merge of these two images (c).

Vit-2 was only partially associated with LDs and the main signal was in total membrane fraction (Fig. 2*C*), suggesting there are at least two types of lipid storage structures in *C. elegans*, Vit containing lipoprotein particles with higher density and lipid droplets with lower density. Their functions and relationship are worth to be investigated.

It is not clear at present why there are so many mitochondrial metabolism proteins (*e.g.* mitochondrial respiratory chain proteins) in our LD proteome (Table I). Similar results have been reported before in LD proteomes for other organisms. It has been proposed that mitochondria, peroxisomes, ER membranes, and endosomes may be physically associated with LDs (5, 34) or may even be continuous with LDs in terms of phospholipid membrane topology (35). Recently, we conducted an interactomic study on interaction between LDs and mitochondria and identified several pairs of proteins that may be involved in this interaction (36).

Our purification and proteomic study has uncovered many bona fide LD-proteins. Using morphological and biochemical analyses, we also identified DHS-3 as a good LD marker protein. These results prove the benefits of purifying LDs and using proteomic approaches over commonly-used genetic approaches to study *C. elegans* LDs. More importantly, this work provides a tool for establishing *in vitro* assays for the study of LDs in *C. elegans*.

As a direct LD detection, our approach may also be used to assess whether the Raman signals of live *C. elegans* captured by Coherent anti-Stokes Raman Spectroscopy and Stimulated Raman Spectroscopy come from LDs or other types of organelles (37–39). For example, the level of colocalization between LD marker proteins and the Raman signals from Coherent anti-Stokes Raman Spectroscopy and Stimulated

Raman Spectroscopy may determine whether these signals can reliably act as a proxy for TAG levels in live *C. elegans*. Furthermore, an *in vitro* assay using isolated LDs and other cellular organelles may help to resolve the issue of the specificity of the Raman signals that are detected by Coherent anti-Stokes Raman Spectroscopy and Stimulated Raman Spectroscopy.

*Acknowledgments*—We would like to thank Dong Tian and Yihong Yang for their technical support, and Dr. Joy Fleming for her critical reading and useful suggestions. Thanks to the Caenorhabditis Genome Center for providing strains and to Developmental Studies Hybridoma Bank for providing antibodies.

* This work was supported by the Ministry of Science and Technology of China (2009CB919000, 2010CB833703, and 2011CBA00900) and the National Natural Science Foundation of China (30971431).

[S] This article contains supplemental Figs. S1 to S3 and Table S1.

‡‡ These authors contributed to this work equally.

** To whom correspondence should be addressed: Institute of Biophysics, Chinese Academy of Sciences, Beijing, 100101, China. Tel.: +86-10-64888517; E-mail: pliu@ibp.ac.cn. College of Life Sciences, Capital Normal University, Beijing, 100048, China. Tel.: +86-10-68903434; Email: soz001@yahoo.com.

REFERENCES

1. Murphy, D. J. (2001) The biogenesis and functions of lipid bodies in animals, plants and microorganisms. *Progress Lipid Res.* **40,** 325–438
2. Martin, S., and Parton, R. G. (2006) Lipid droplets: a unified view of a dynamic organelle. *Mol. Cell Biol.* **7,** 373–378
3. Farese, R. V., Jr., and Walther, T. C. (2009) Lipid droplets finally get a little R-E-S-P-E-C-T. *Cell* **139,** 855–860
4. Goodman, J. M. (2009) Demonstrated and inferred metabolism associated with cytosolic lipid droplets. *J. Lipid Res.* **50,** 2148–2156
5. Zehmer, J. K., Huang, Y., Peng, G., Pu, J., Anderson, R. G., and Liu, P. (2009) A role for lipid droplets in inter-membrane lipid traffic. *Proteomics* **9,** 914–921
6. Liu, P., Bartz, R., Zehmer, J. K., Ying, Y. S., Zhu, M., Serrero, G., and Anderson, R. G. (2007) Rab-regulated interaction of early endosomes with lipid droplets. *Biochim. Biophys. Acta* **1773,** 784–793
7. Liu, P., Bartz, R., Zehmer, J. K., Ying, Y., and Anderson, R. G. (2008) Rab-regulated membrane traffic between adiposomes and multiple endomembrane systems. *Methods Enzymol.* **439,** 327–337
8. Szymanski, K. M., Binns, D., Bartz, R., Grishin, N. V., Li, W. P., Agarwal, A. K., Garg, A., Anderson, R. G., and Goodman, J. M. (2007) The lipodystrophy protein seipin is found at endoplasmic reticulum lipid droplet junctions and is important for droplet morphology. *Proc. Natl. Acad. Sci. U. S. A.* **104,** 20890–20895
9. Kimmel, A. R., Brasaemle, D. L., McAndrews-Hill, M., Sztalryd, C., and Londos, C. (2010) Adoption of PERILIPIN as a unifying nomenclature for the mammalian PAT-family of intracellular lipid storage droplet proteins. *J. Lipid Res.* **51,** 468–471
10. Athenstaedt, K., Zweytick, D., Jandrositz, A., Kohlwein, S. D., and Daum, G. (1999) Identification and characterization of major lipid particle proteins of the yeast Saccharomyces cerevisiae. *J. Bacteriol.* **181,** 6441–6448
11. Wu, C. C., Howell, K. E., Neville, M. C., Yates, J. R., 3rd, and McManaman, J. L. (2000) Proteomics reveal a link between the endoplasmic reticulum and lipid secretory mechanisms in mammary epithelial cells. *Electrophoresis* **21,** 3470–3482
12. Liu, P., Ying, Y., Zhao, Y., Mundy, D. I., Zhu, M., and Anderson, R. G. (2004) Chinese hamster ovary K2 cell lipid droplets appear to be metabolic organelles involved in membrane traffic. *J. Biol. Chem.* **279,** 3787–3792
13. Brasaemle, D. L., Dolios, G., Shapiro, L., and Wang, R. (2004) Proteomic analysis of proteins associated with lipid droplets of basal and lipolytically stimulated 3T3-L1 adipocytes. *J. Biol. Chem.* **279,** 46835–46842
14. Fujimoto, Y., Itabe, H., Sakai, J., Makita, M., Noda, J., Mori, M., Higashi, Y., Kojima, S., and Takano, T. (2004) Identification of major proteins in the lipid droplet-enriched fraction isolated from the human hepatocyte cell line HuH7. *Biochim. Biophys. Acta* **1644,** 47–59
15. Umlauf, E., Csaszar, E., Moertelmaier, M., Schuetz, G. J., Parton, R. G., and Prohaska, R. (2004) Association of stomatin with lipid bodies. *J. Biol. Chem.* **279,** 23699–23709
16. Bartz, R., Zehmer, J. K., Zhu, M., Chen, Y., Serrero, G., Zhao, Y., and Liu, P. (2007) Dynamic activity of lipid droplets: protein phosphorylation and GTP-mediated protein translocation. *J. Proteome Res.* **6,** 3256–3265
17. Bartz, R., Li, W. H., Venables, B., Zehmer, J. K., Roth, M. R., Welti, R., Anderson, R. G., Liu, P., and Chapman, K. D. (2007) Lipidomics reveals that adiposomes store ether lipids and mediate phospholipid traffic. *J. Lipid Res.* **48,** 837–847
18. Beller, M., Riedel, D., Jänsch, L., Dieterich, G., Wehland, J., Jackle, H., and Kühnlein, R. P. (2006) Characterization of the Drosophila lipid droplet subproteome. *Mol. Cell. Proteomics* **5,** 1082–1094
19. Cermelli, S., Guo, Y., Gross, S. P., and Welte, M. A. (2006) The lipid-droplet proteome reveals that droplets are a protein-storage depot. *Current Biol.* **16,** 1783–1795
20. Zhang, S., Du, Y., Wang, Y., and Liu, P. (2010) Lipid Droplet—A Cellular Organelle for Lipid Metabolism. *Acta Biophys. Sin.* **26,** 97–105
21. Zhang, S. O., Box, A. C., Xu, N., Le Men, J., Yu, J., Guo, F., Trimble, R., and Mak, H. Y. (2010) Genetic and dietary regulation of lipid droplet expansion in Caenorhabditis elegans. *Proc. Natl. Acad. Sci. U. S. A.* **107,** 4640–4645
22. Zhang, S. O., Trimble, R., Guo, F., and Mak, H. Y. (2010) Lipid droplets as ubiquitous fat storage organelles in C. elegans. *BMC Cell Biol.* **11,** 96
23. Schroeder, L. K., Kremer, S., Kramer, M. J., Currie, E., Kwan, E., Watts, J. L., Lawrenson, A. L., and Hermann, G. J. (2007) Function of the Caenorhabditis elegans ABC transporter PGP-2 in the biogenesis of a lysosome-related fat storage organelle. *Mol. Biol. Cell* **18,** 995–1008
24. Brooks, K. K., Liang, B., and Watts, J. L. (2009) The influence of bacterial diet on fat storage in C. elegans. *PloS One* **4,** e7545
25. O'Rourke, E. J., Soukas, A. A., Carr, C. E., and Ruvkun, G. (2009) C. elegans major fats are stored in vesicles distinct from lysosome-related organelles. *Cell Metabolism* **10,** 430–435
26. Suzuki, M., Shinohara, Y., Ohsaki, Y., and Fujimoto, T. (2011) Lipid droplets: size matters. *J. Elect. Micros.* **60,** S101–116
27. Brasaemle, D. L., and Wolins, N. E. (2012) Packaging of fat: an evolving model of lipid droplet assembly and expansion. *J. Biol. Chem.* **287,** 2273–2279
28. Szklarczyk, D., Franceschini, A., Kuhn, M., Simonovic, M., Roth, A., Minguez, P., Doerks, T., Stark, M., Muller, J., Bork, P., Jensen, L. J., and von Mering, C. (2011) The STRING database in 2011: functional interaction networks of proteins, globally integrated and scored. *Nucleic Acids Res.* **39,** D561–568
29. Narbonne, P., and Roy, R. (2009) Caenorhabditis elegans dauers need LKB1/AMPK to ration lipid reserves and ensure long-term survival. *Nature* **457,** 210–214
30. Kage-Nakadai, E., Kobuna, H., Kimura, M., Gengyo-Ando, K., Inoue, T., Arai, H., and Mitani, S. (2010) Two very long chain fatty acid acyl-CoA synthetase genes, acs-20 and acs-22, have roles in the cuticle surface barrier in Caenorhabditis elegans. *PloS One* **5,** e8857
31. Ozeki, S., Cheng, J., Tauchi-Sato, K., Hatano, N., Taniguchi, H., and Fujimoto, T. (2005) Rab18 localizes to lipid droplets and induces their close apposition to the endoplasmic reticulum-derived membrane. *J. Cell Sci.* **118,** 2601–2611
32. Guo, Y., Walther, T. C., Rao, M., Stuurman, N., Goshima, G., Terayama, K., Wong, J. S., Vale, R. D., Walter, P., and Farese, R. V. (2008) Functional genomic screen reveals genes involved in lipid-droplet formation and utilization. *Nature* **453,** 657–661
33. Kubagawa, H. M., Watts, J. L., Corrigan, C., Edmonds, J. W., Sztul, E., Browse, J., and Miller, M. A. (2006) Oocyte signals derived from polyunsaturated fatty acids control sperm recruitment in vivo. *Nat. Cell Biol.* **8,** 1143–1148
34. Murphy, S., Martin, S., and Parton, R. G. (2009) Lipid droplet-organelle interactions; sharing the fats. *Biochim. Biophys. Acta* **1791,** 441–447
35. Goodman, J. M. (2008) The gregarious lipid droplet. *J. Biol. Chem.* **283,** 28005–28009
36. Pu, J., Ha, C. W., Zhang, S., Jung, J. P., Huh, W. K., and Liu, P. (2011) Interactomic study on interaction between lipid droplets and mitochondria. *Protein & cell* **2,** 487–496

37. Hellerer, T., Axäng, C., Brackmann, C., Hillertz, P., Pilon, M., and Enejder, A. (2007) Monitoring of lipid storage in Caenorhabditis elegans using coherent anti-Stokes Raman scattering (CARS) microscopy. *Proc. Natl. Acad. Sci. U. S. A.* **104,** 14658–14663
38. Yen, K., Le, T. T., Bansal, A., Narasimhan, S. D., Cheng, J. X., and Tissenbaum, H. A. (2010) A comparative study of fat storage quantitation in nematode Caenorhabditis elegans using label and label-free methods. *PloS one* **5**, e12810
39. Zhang, H., Wang, Y., Li, J., Yu, J., Pu, J., Li, L., Zhang, H., Zhang, S., Peng, G., Yang, F., and Liu, P. (2011) Proteome of skeletal muscle lipid droplet reveals association with mitochondria and apolipoprotein a-I. *J. Proteome Res.* **10,** 4757–4768
40. Turró, S., Ingelmo-Torres, M., Estanyol, J. M., Tebar, F., Fernández, M. A., Albor, C. V., Gaus, K., Grewal, T., Enrich, C., and Pol, A. (2006) Identification and characterization of associated with lipid droplet protein 1: A novel membrane-associated protein that resides on hepatic lipid droplets. *Traffic* **7,** 1254–1269
41. Sato, S., Fukasawa, M., Yamakawa, Y., Natsume, T., Suzuki, T., Shoji, I., Aizaki, H., Miyamura, T., and Nishijima, M. (2006) Proteomic profiling of lipid droplet proteins in hepatoma cell lines expressing hepatitis C virus core protein. *J. Biochem.* **139,** 921–930
42. Wan, H. C., Melo, R. C., Jin, Z., Dvorak, A. M., and Weller, P. F. (2007) Roles and origins of leukocyte lipid bodies: proteomic and ultrastructural studies. *FASEB J.* **21,** 167–178
43. Katavic, V., Agrawal, G. K., Hajduch, M., Harris, S. L., and Thelen, J. J. (2006) Protein and lipid composition analysis of oil bodies from two Brassica napus cultivars. *Proteomics* **6,** 4586–4598
44. Kim, S. C., Chen, Y., Mirza, S., Xu, Y., Lee, J., Liu, P., and Zhao, Y. (2006) A clean, more efficient method for in-solution digestion of protein mixtures without detergent or urea. *J. Proteome Res.* **5,** 3446–3452
45. Bouchoux, J., Beilstein, F., Pauquai, T., Guerrera, I. C., Chateau, D., Ly, N., Alqub, M., Klein, C., Chambaz, J., Rousset, M., Lacorte, J. M., Morel, E., and Demignot, S. (2011) The proteome of cytosolic lipid droplets isolated from differentiated Caco-2/TC7 enterocytes reveals cell-specific characteristics. *Biol. Cell* **103,** 499–517
46. Ding, Y., Yang, L., Zhang, S., Wang, Y., Du, Y., Pu, J., Peng, G., Chen, Y., Zhang, H., Yu, J., Hang, H., Wu, P., Yang, F., Yang, H., Steinbuchel, A., and Liu, P. (2011) Identification of the major functional proteins of Prokaryotic lipid droplets. *J. Lipid Res.* **53,** 399–411